



Preparation and Characterization of Zirconia Nanomaterial as a Molybdenum-99 Adsorbent

Marlina, E. Sarmini, Herlina, Sriyono, I. Saptiama, H. Setiawan and Kadarisman

Center for Radioisotope and Radiopharmaceutical Technology, National Nuclear Energy Agency

Puspiptek, Serpong, Tangerang 15314, Indonesia

ARTICLE INFO

Article history:

Received 2 November 2015

Received in revised form 9 September 2016

Accepted 20 September 2016

Keywords:

Nanozirconia

Sol-gel method

Adsorption capacity

Molybdenum-99

ABSTRACT

The present study deals with the synthesis and characterization of ZrO_2 nanomaterial which can be used as an adsorbent for Molybdenum-99 (^{99}Mo). The adsorbent can potentially be utilized as the material for $^{99}\text{Mo}/^{99\text{m}}\text{Tc}$ generator column. Using the sol-gel method, monoclinic nanocrystalline zirconia was synthesized from zirconium oxychloride in isopropyl alcohol reacted with ammonium hydroxide solution in isopropyl alcohol resulting in a white gel. The gel was subsequently refluxed for 12 hours at $\sim 95^\circ\text{C}$ and pH at ~ 4 and then dried at 100°C . The drying gel was then calcined at 600°C for two hours. Meanwhile the orthorhombic nanocrystalline zirconia was obtained by reacting zirconium oxychloride solution with 2.5 M ammonium hydroxide solution which resulted in a white gel. The gel was then refluxed for 24 hours at $\sim 95^\circ\text{C}$ and pH at ~ 11 and then dried at 100°C . The drying gel was then calcined at 600°C for two hours. These materials were characterized using FT-IR spectroscopy, X-ray diffraction (XRD), and Transmission Electron Microscope (TEM). The Scherrer method is used for determination of crystallite size. The FT-IR spectra for both materials show absorption peak at $450\text{--}500\text{ cm}^{-1}$ which are attributed to Zr-O bond. The XRD pattern of monoclinic nanocrystalline form shows crystalline peaks at 2θ regions of 28.37° , 31.65° , 34° , 36° and 50.3° with average crystallite size of 2.68 nm. Meanwhile, the XRD pattern of orthorhombic nanocrystalline form shows crystalline peaks at 2θ regions of 30° , 35° , 50° and 60° with average crystallite size of 0.98 nm. The TEM micrograph indicates that the zirconia nanomaterials prepared were quite uniform in size and shape.

© 2017 Atom Indonesia. All rights reserved

INTRODUCTION

The $^{99}\text{Mo}/^{99\text{m}}\text{Tc}$ generator is a radionuclide generator system that is highly needed to produce the Technetium-99 ($^{99\text{m}}\text{Tc}$) radionuclide. This radionuclide is used for clinical applications, especially for diagnostic imaging in nuclear medicine. The $^{99\text{m}}\text{Tc}$ -radiopharmaceuticals are used for more than 80 % of diagnostic imaging procedures world-wide every year [1].

The principle of a radionuclide generator is the decay-growth relationship between a long-lived parent radionuclide and a short-lived daughter radionuclide (as decay product), which can be readily separated by the column chromatography technique. The advantages of the radionuclide generator are that it is easy to carry, is cheap, produces daughter radionuclide in a high specific activity, and can be applied for diagnosis or therapy at locations/sites far from the isotope production facilities [2].

Figure 1 depicts radionuclide generator components. The chromatography column used in $^{99}\text{Mo}/^{99\text{m}}\text{Tc}$ generator contains an adsorbent that can

*Corresponding author.

E-mail address: marlina@batan.go.id

DOI: <http://dx.doi.org/10.17146/aij.2017.587>

adsorb ^{99}Mo radionuclide. ^{99}Mo radionuclide (as parent radionuclide) decays by emitting β particles, metastable $^{99\text{m}}\text{Tc}$ radionuclide (87.5 %), and ^{99}Tc (12.5 %). Furthermore, $^{99\text{m}}\text{Tc}$ decays to ^{99}Tc with a half-life of 6.02 hours and a gamma emission of 140.5 keV. The daughter radionuclide $^{99\text{m}}\text{Tc}$ is separated from parent radionuclide ^{99}Mo using sterile saline for elution of $^{99\text{m}}\text{Tc}$ as $^{99\text{m}}\text{Tc}(\text{VII})\text{O}_4^-$ pertechnetate anion [3].

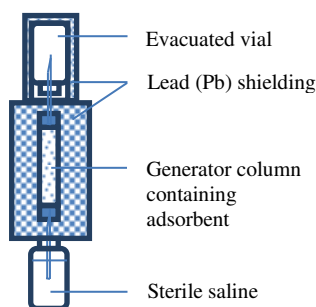


Fig.1. Radionuclide generator components.

The adsorbent commonly used in $^{99}\text{Mo}/^{99\text{m}}\text{Tc}$ generator is alumina (Al_2O_3). Alumina has limited Mo adsorption capacity, which is ~ 20 mg Mo/g of alumina [4]. The use of alumina requires ^{99}Mo of high specific activity. The high specific activity ^{99}Mo can only be produced from fission product of Uranium-235 (^{235}U). Since last decade, the use of highly-enriched uranium (HEU) either for fuel of research reactor or ^{99}Mo and $^{99\text{m}}\text{Tc}$ production, is strictly bounded as a mandate from US Congress.

Subsequently, ^{99}Mo production is carried out by thermal neutron activation of natural Mo in nuclear reactors, based on $^{98}\text{Mo}(\text{n},\gamma)^{99}\text{Mo}$ reaction [3]. The ^{99}Mo radionuclide resulting from such a reaction is a radionuclide of the same element as the target nuclide, so the two of them could not be chemically separated. Subsequently, the resulting ^{99}Mo is a carrier-added radionuclide which has low specific activity (< 10 Ci/g of Mo) [3].

Therefore, there are needs to develop some adsorbents which can be used to adsorb neutron-activated ^{99}Mo . The Center for Radioisotope and Radiopharmaceutical Technology (PTRR), BATAN, collaborating with JAEA/Chiyoda, has developed an adsorbent, namely *Poly Zirconium Compound* (PZC). This adsorbent has been used for $^{99}\text{Mo}/^{99\text{m}}\text{Tc}$ generator at ^{99}Mo activity of > 5 Ci; the Mo adsorption capacity achieved was up to ~ 250 mg Mo/g of PZC [5].

PTRR BATAN has also been developing a zirconium-based material (ZBM) as a matrix for $^{99}\text{Mo}/^{99\text{m}}\text{Tc}$ generator column using neutron activated ^{99}Mo . The ZBM has achieved an Mo

adsorption capacity of up to ~ 193 mg Mo/g of ZBM [6].

The mechanism of ^{99}Mo adsorption into the ZBM was studied by Rohadi *et al.* It was found that the molybdate ion adsorption into the ZBM followed the ion exchange mechanism with Cl^- ions contained in the material. Also, to increase the yield of $^{99\text{m}}\text{Tc}$ eluate from the generator, a sodium hypochlorite solution (NaOCl) was used as an oxidizing agent [7]. The yield of $^{99\text{m}}\text{Tc}$ eluate can be increased by up to 70 % under optimal conditions using NaOCl 3 % [8].

Other adsorbents developed for $^{99}\text{Mo}/^{99\text{m}}\text{Tc}$ generator are functionalized alumina and titanium polymer. These materials have higher Mo adsorption capacity than alumina (> 250 mg Mo/g of adsorbent) [4].

Chakravarty *et al.* have developed several nanomaterial adsorbents for radionuclide generator applications. They are polymer embedded nanocrystalline titania (TiP), mixed phase nano-zirconia (nano- ZrO_2) tetragonal nano-zirconia (t-ZrO_2), nanocrystalline alumina ($\gamma\text{-Al}_2\text{O}_3$), and nano-ceria-polyacrylonitrile composite ($\text{CeO}_2\text{-PAN}$) [2,9,10].

A nanomaterial is an object with size of < 100 nm. The small size of its particles can increase its surface energy. Nanomaterials have unique physical and chemical properties. Atoms on nanomaterial surfaces have high chemical activity and adsorption capacity to metal ions. Therefore, nanomaterials could adsorb many substances including trace metals and polar organic compounds [11].

In connection with Mo adsorption, nanomaterials can increase the interaction with molybdate ion on its surface, so that it increases Mo adsorption capacity [2]. Nanomaterials have the potential to be developed as Mo adsorbents for $^{99}\text{Mo}/^{99\text{m}}\text{Tc}$ generator columns. The advantages of the use of nanomaterials as adsorbents in a radionuclide generator column include high adsorption capability, selectivity towards certain radionuclide, favorable radiation, and mechanical and thermal stability, as well as possibility for regeneration and reusability [2].

The objectives of this study are to synthesize and characterize zirconia nanomaterials and prepare them as adsorbents for ^{99}Mo radionuclide that will be applied for $^{99}\text{Mo}/^{99\text{m}}\text{Tc}$ generator column.

EXPERIMENTAL METHODS

In this study two zirconia nanomaterials was prepared, namely zirconia nanomaterial A and

zirconia nanomaterial B. The method used in this experiment is the sol-gel method [12].

In order to characterize the nanomaterials and understand their properties, Fourier transform infrared spectroscopy (FT-IR), powder X-ray diffraction (XRD), and transmission electron microscopy (TEM) analyses were employed. The HighScorePlus software is employed for crystallographic analysis.

Materials and equipment

Reagents including $\text{ZrOCl}_2 \cdot 8\text{H}_2\text{O}$, isopropyl alcohol, ammonia 32 %, and pH-indicator strips pH 0-14 Universal indicator was purchased from Merck, while aquabidest and demineralized water were purchased from a local company, IPHA, Bandung, Indonesia. All reagents used were analytical grade.

The equipment used consisted of beaker glasses, hot plate stirrers, evaporating dishes, thermometers, and a furnace (Raypa®). Characterizations were carried out by an Alpha FT-IR spectrometer (Bruker) which spectra were recorded in the range of $450\text{--}4,000\text{ cm}^{-1}$, a JEOL JEM-1400 120 kV transmission electron microscope, and a Miniflex 600 X-ray diffraction system.

Synthesis of zirconia nanomaterial A

The synthesis of zirconia nanomaterial A is based on controlled hydrolysis reaction of zirconium oxychloride in isopropyl alcohol medium. $\text{ZrOCl}_2 \cdot 8\text{H}_2\text{O}$ was dissolved in 80 % isopropyl alcohol, then a 20 % ammonium hydroxide solution (in 80 % isopropyl alcohol medium) was slowly added. The mixture was stirred vigorously without heating until white gel was formed. The formed gel was then refluxed at $\sim 95^\circ\text{C}$ for 12 hours at a pH of ~ 4 . Afterward, the gel was kept at room temperature for 24 hours. The gel was washed with demineralized water, dried at 100°C and then followed by calcination at 600°C for two hours.

Synthesis of zirconia nanomaterial B

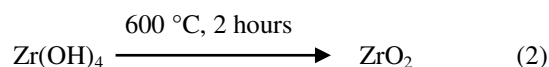
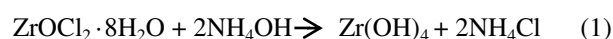
$\text{ZrOCl}_2 \cdot 8\text{H}_2\text{O}$ was dissolved in aquabidest. The zirconium solution was added into 2.5 M ammonium hydroxide solution with vigorous stirring, until white gel was formed. The formed gel was maintained at a pH of ~ 11 by adding of 2.5 M ammonium hydroxide solution. The gel was then washed with demineralized water until free of Cl^-

ions. Precipitation reaction using 0.1 M AgNO_3 solution was carried out to reveal the presence of the Cl^- ion. Subsequently, the gel was refluxed at $\sim 95^\circ\text{C}$ for 12 hours at a pH of ~ 11 . Furthermore, the gel was kept at room temperature for 24 hours. The gel was then washed with demineralized water, dried at 100°C and then followed by calcination at 600°C for two hours.

RESULTS AND DISCUSSION

Zirconia nanomaterial A

The reaction between zirconium oxychloride and ammonium hydroxide solution in 80 % isopropyl alcohol medium, leads to the formation of white gel, that is zirconium hydroxide, $\text{Zr}(\text{OH})_4$ [13]. After the dried gel was calcined at 600°C for two hours, it turned into a white powder that is presumably zirconium oxide (zirconia). The chemical reaction is as follows:



The characterization of zirconia nanomaterial A was carried out by comparing FT-IR spectra of $\text{ZrOCl}_2 \cdot 8\text{H}_2\text{O}$ as a reactant, standard ZrO_2 (Atomergic Chemetals Corp.), and zirconia nanomaterial A, as shown in Fig. 2.

Figure 2(a) shows the FT-IR spectrum of $\text{ZrOCl}_2 \cdot 8\text{H}_2\text{O}$. The spectrum contains absorption peak at 1589 cm^{-1} for bending vibration of the O-H groups of the free H_2O , and absorption peaks at $450\text{--}500\text{ cm}^{-1}$ that are attributed to the Zr-O bond [14]. Figure 2(b) is the FT-IR spectrum of standard ZrO_2 , showing absorption peaks at $450\text{--}500\text{ cm}^{-1}$ that are attributed to the Zr-O bond. By comparing the FT-IR spectrum of zirconia nanomaterial A (Fig. 2(c)) to Fig. 2(a) and 2(b), based on the absence of absorption peak of the O-H group of the free H_2O and the similarity with the spectrum of standard ZrO_2 , it is concluded that the prepared zirconia nanomaterial A is a zirconia compound.

Furthermore, the prepared zirconia nanomaterial A was characterized using TEM to study the size and morphology of the material. The TEM images of zirconia nanomaterial A are shown in Fig. 3.

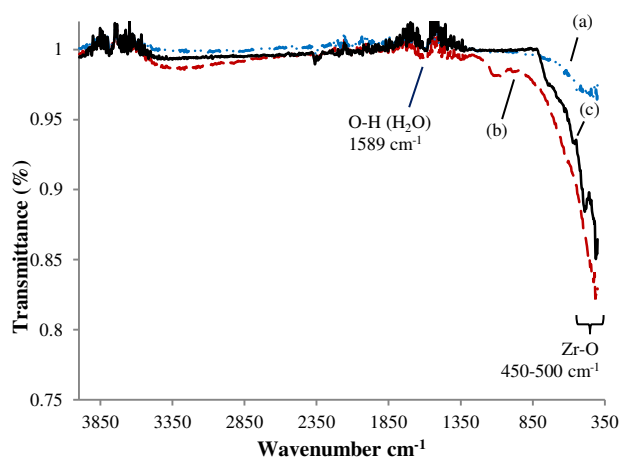


Fig. 2. FT-IR spectra of: (a) $\text{ZrOCl}_2 \cdot 8\text{H}_2\text{O}$, (b) standard zirconia, (c) zirconia nanomaterial A.

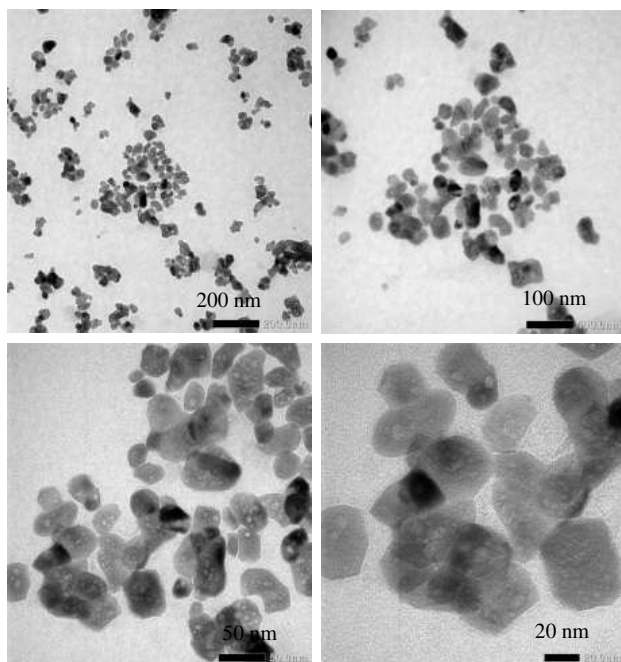


Fig. 3. Representative TEM images of particle morphology of the zirconia nanomaterial A.

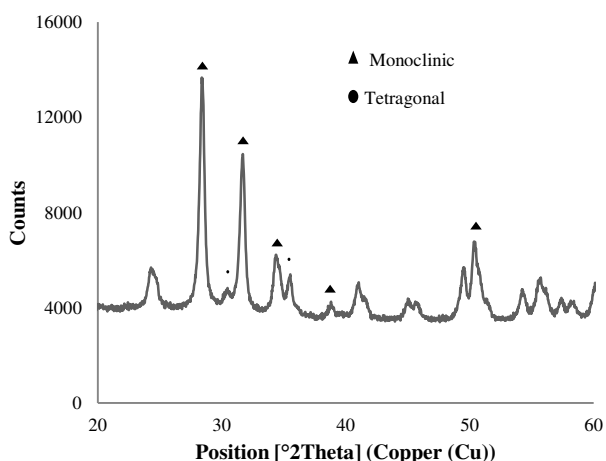


Fig. 4. XRD pattern of zirconia nanomaterial A.

Figure 3 shows that the prepared zirconia nanomaterial A is in a crystalline form. It can also be observed that the particles are quite uniform in size and shape, with average particle size of less than 20 nm. The XRD pattern of prepared zirconia nanomaterial A is shown in Fig. 4.

The qualitative analysis of the zirconia nanomaterial A using the HighScore Plus software conforms that the material consists of two phases, namely baddeleyite and zirconium oxide phase. In baddeleyite phase (92.4 %), crystalline peaks appear at 2θ ($^\circ$) regions of 28.37° , 31.65° , 34° , 36° and 50.3° , with lattice constants of $a = 5.1200 \text{ \AA}$, $b = 5.2160 \text{ \AA}$, $c = 5.2810 \text{ \AA}$, $\alpha = \gamma = 90^\circ$, and $\beta = 99.01^\circ$. The space group of the crystal is $P 1 2_1/c 1$ with space group number of 14. This XRD pattern is typical for monoclinic lattice in nanocrystalline zirconia. In zirconium oxide phase (7.6 %), crystalline peaks appear at 2θ regions of 30° and 35° , with lattice constants of $a = b = 3.5870 \text{ \AA}$, $c = 5.1670 \text{ \AA}$ and $\alpha = \beta = \gamma = 90^\circ$. The space group of the crystal is $P 42/n m c$ with space group number of 137. This XRD pattern is typical for tetragonal lattice in nanocrystalline zirconia [15]. The Debye-Scherrer equation is used for determination of crystallite size. The equation can be written as:

$$D = \frac{K\lambda}{\beta \cos \theta} \quad (3)$$

where:

- D is the crystallite size.
- K is the shape factor ($K = 0.9$, assuming spherical crystallites).
- λ is the X-ray wavelength (1.54056 \AA).
- β is the full width at half maximum (FWHM) (rad).
- θ is the Bragg angle (rad).

Table 1. Crystallite size of the zirconia nanomaterial A.

2θ ($^\circ$)	θ (rad)	FWHM (β) rad	D (nm)
28.3760	0.2476	0.009265	2.694
31.6433	0.2761	0.009405	2.674

Based on the Table 1, the prepared zirconia material A has an average crystallite size of 2.68 nm.

Zirconia nanomaterial B

In the preparation of the zirconia material B, the reaction between zirconium oxychloride and ammonium hydroxide solution was carried out in

water. After the dried gel was calcined at 600 °C for two hours, it turned into a light blue powder that is presumably zirconium oxide (zirconia). The reaction occurred in the preparation of the zirconia material B and is similar to the synthesis of zirconia nanomaterial A given by equations (1) and (2).

The characterization of the prepared zirconia nanomaterial B was carried out by comparing the FT-IR spectrum of standard ZrO_2 (Fig. 2(b)) to the FT-IR spectrum of zirconia nanomaterial B (Fig. 5). Figure 5 shows absorption peaks at 1010 cm^{-1} and $450\text{--}500\text{ cm}^{-1}$ which are attributed to the Zr-O bond [14] and the spectrum is similar to that of the standard ZrO_2 ; thus, one can conclude that the prepared zirconia nanomaterial B is a zirconia compound.

The TEM images of the prepared zirconia nanomaterial B is shown in Fig. 6. It indicates that the material is in a crystalline form. It is also observed that the particles are quite uniform in size and shape, with an average particle size of less than 20 nm. The XRD pattern of the prepared zirconia nanomaterial B is shown in Fig. 7.

The qualitative analysis of the zirconia nanomaterial B using the HighScore Plus software confirms that the material consists of baddeleyite phase (100 %), and the crystalline peaks appear at 2θ regions of 30° , 35° , 50° and 60° , with lattice constants of $a = 4.9940\text{ \AA}$, $b = 5.2290\text{ \AA}$, $c = 5.0460\text{ \AA}$, and $\alpha = \beta = \gamma = 90^\circ$. The space group of the crystal is $Pb\bar{c}m$ with space group number of 57. This XRD pattern is typical for the orthorhombic lattice in nanocrystalline zirconia [16]. By using equation (3), it is found the prepared zirconia material B has an average crystallite size of 0.98 nm.

Chakravarty *et al.* have studied the preparation of nanocrystalline zirconia, namely mixed phase (monoclinic-tetragonal) and tetragonal nanocrystalline zirconia. The former has a crystallite size of 15 nm and is used for $^{188}\text{W}/^{188}\text{Re}$ generator. The latter has a crystallite size of 7 nm and is used for $^{99}\text{Mo}/^{99\text{m}}\text{Tc}$ generator. The tetragonal nanocrystalline zirconia has a ^{99}Mo adsorption capacity of 250 mg Mo/g [2]. Meanwhile, this study has resulted in the orthorhombic nanocrystalline zirconia which has crystallite size of 0.98 nm. Because the orthorhombic nanocrystalline zirconia has a smaller crystallite size than mixed-phase (monoclinic-tetragonal) or tetragonal nanocrystalline zirconia, it is expected to have a greater ^{99}Mo adsorption capacity. Therefore, the orthorhombic nanocrystalline zirconia will give better results as a ^{99}Mo adsorbent.

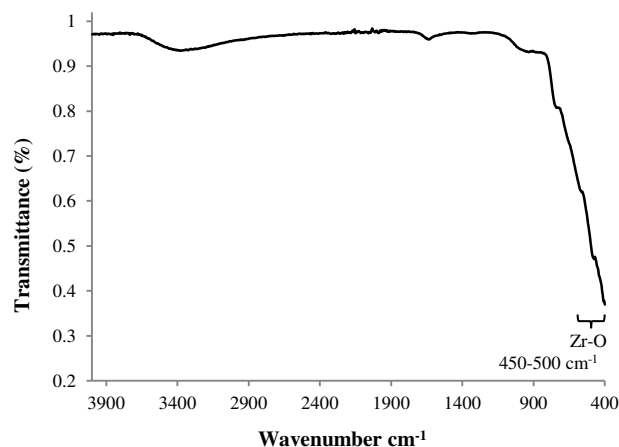


Fig. 5. FT-IR spectrum of zirconia nanomaterial B.

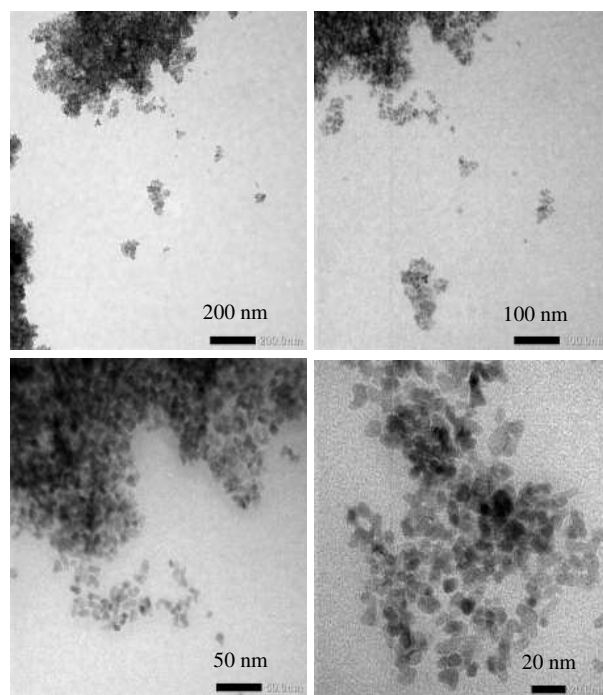


Fig. 6. Representative TEM images of particle morphology of the zirconia nanomaterial B.

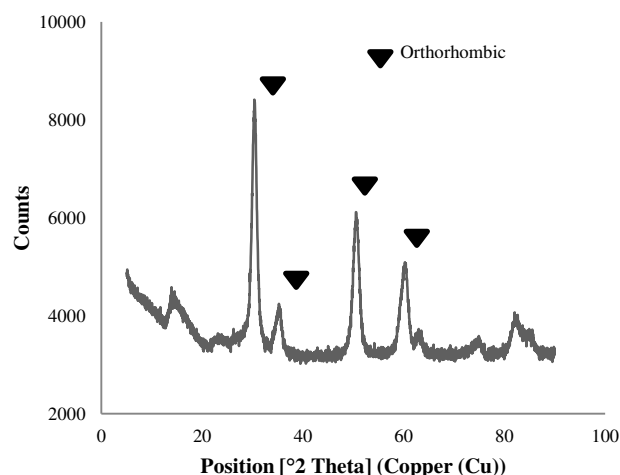


Fig. 7. XRD pattern of zirconia nanomaterial B.

CONCLUSION

In the present study, nanocrystalline zirconia materials have been synthesized with monoclinic (92.4 %) and tetragonal (7.6 %) crystalline structures having average crystallite size of ~17 nm, and nanocrystalline zirconia material with orthorhombic (100 %) crystalline structure having average crystallite size of ~0.98 nm.

Furthermore, these prepared zirconia nanomaterials will be employed to determine the Mo adsorption capacity, to understand whether these zirconia nanomaterials can be applied as adsorbent for $^{99}\text{Mo}/^{99\text{m}}\text{Tc}$ generator.

ACKNOWLEDGMENT

This work is fully supported by the Indonesian government funding (DIPA 2015), through the National Nuclear Energy Agency, BATAN. The author would like to thank Drs. Hotman Lubis, as the head of Radioisotope Technology Division of the Center for Radioisotope and Radiopharmaceutical Technology for the encouragement and support, Siska Febriana for XRD data analysis, and Enny Lestari and Abidin for technical assistances.

REFERENCES

1. V.S. Le, Z.P. Do, M.K. Le *et al.*, *Molecule* **19** (2014) 7714.
2. R. Chakravarty and A. Dash, *J. Radioanal. Nucl. Chem.* **299** (2014) 741.
3. I. Zolle, *Technetium-99m Pharmaceuticals Preparation And Quality Control in Nuclear Medicine*, Springer Berlin Heidelberg, New York (2007) 7.
4. V.S. Le, *Science and Technology of Nuclear Installations* **2014** (2014) 41.
5. H.G. Adang, A. Mutalib, L. Hotman *et al.*, *Performance of $^{99}\text{Mo}/^{99\text{m}}\text{Tc}$ Generator Based PZC (Poly Zirconium Compound) using ^{99}Mo via Natural Molybdenum-Nutron Activated with 5 Ci ^{99}Mo activity*, *Proceeding of National Conference on Basic Research and Nuclear Technology* (2011) 44. (in Indonesian)
6. I. Saptiama, Sriyono and Herlina, *JFN* **6** (2012) 114. (in Indonesian)
7. R. Awaludin, A.H. Gunawan, H. Lubis *et al.*, *J. Radioanal. Nucl. Chem.* **303** (2015) 1481.
8. I. Saptiama, Marlina, E. Sarmini *et al.*, *Atom Indonesia* **41** (2015) 103.
9. A. Dash and R. Chakravarty, *RSC Adv.* **4** (2014) 42779.
10. R. Chakravarty, R. Ram, K.C. Jagdeesan *et al.*, *Chromatographia* **74** (2011) 531.
11. M. Khajeh, S. Laurent, K. Dastafkan, *Chem. Rev.* **113** (2013) 7728.
12. K.V. Vimalnath, S. Priyalata, S. Chakraborty *et al.*, *J. Radioanal. Nucl. Chem.* **302** (2014) 1245.
13. E. Susiantini, *J. Iptek Ganendra* **16** (2013) 18. (in Indonesian)
14. M. Ranjbar, M. Yousefi, M. Lahooti *et al.*, *Int. J. Nanosci. Nanotechnol* **8** (2012) 191.
15. S. Rifki, S.P. Bambang, S. Suhandha *et al.*, *J. Ceram. Proc. Res.* **12** (2011) 110.
16. O. Ohtaka, T. Yamanaka, S. Kume *et al.*, *J. Am. Ceram. Soc.* **74** (1991) 505.